

Metastable behavior of the spin- s Ising and Blume-Capel ferromagnets: A Monte Carlo study

Moumita Naskar and Muktish Acharyya^{*}

Department of Physics, Presidency University, 86/1 College Street, Kolkata-700073, India

Erol Vatansever[†]

Department of Physics, Dokuz Eylül University, TR-35160 Izmir, Turkey and Centre for Fluid and Complex Systems, Coventry University, Coventry CV1 5FB, United Kingdom

Nikolaos G. Fytas[†]

Centre for Fluid and Complex Systems, Coventry University, Coventry CV1 5FB, United Kingdom



(Received 11 March 2021; accepted 14 June 2021; published 7 July 2021)

We present an extensive Monte Carlo investigation of the metastable lifetime through the reversal of the magnetization of spin- s Ising and Blume-Capel models, where $s = \{1/2, 1, 3/2, 2, 5/2, 3, 7/2\}$. The mean metastable lifetime (or reversal time) is studied as a function of the applied magnetic field, and for both models it is found to obey the Becker-Döring theory, as was initially developed for the case of an $s = 1/2$ Ising ferromagnet within the classical nucleation theory. Moreover, the decay of the metastable volume fraction nicely follows Avrami's law for all values of s and for both models considered.

DOI: [10.1103/PhysRevE.104.014107](https://doi.org/10.1103/PhysRevE.104.014107)

I. INTRODUCTION

The metastable behavior of a ferromagnet is an interesting field of modern research [1]. It is well known today that the lifetime of a metastable state plays an important role in the technological area of magnetic recording [2]. The whole problem dates back to 1935, where the classical theory of nucleation was developed by Becker and Döring [3], predicting the growth of supercritical droplets. These predictions of the different regimes of such growth depending on the magnitude of the applied magnetic field were successfully verified by extensive Monte Carlo simulation [4] in Ising ferromagnets. Needless to say, the fruit-fly model of statistical physics, i.e., the Ising model, is a prototype system that allows for a clear investigation of all these phenomena.

In more recent years, several interesting complications around this fundamental problem have been proposed and clarified. In particular, the effects of a random magnetic field were investigated in Ref. [5], where the cutoff value of the random field was predicted to deviate from the Becker-Döring theory. The role of a uniform anisotropy in metastability of the spin-1 Blume-Capel ferromagnet was studied in Ref. [6], and a scaling law relating to the stable magnetization, applied field, and anisotropy was proposed. Also, the decay of a metastable state was found to follow Avrami's law [7]. Finally, the spatial variation of the anisotropy (graded- and steplike over the lattice) to tune the switching time has been proposed in Ref. [8], again regarding the anisotropic Blume-Capel ferromagnet.

All studies mentioned above focused on the standard spin- $1/2$ Ising and spin-1 Blume-Capel ferromagnets. This is of no surprise as the Becker-Döring theory was originally proposed for spin- $1/2$ ferromagnets. In the current paper, we address the obvious next-step question of whether the predictions of classical nucleation theory can be observed at any spin- s Ising-type ferromagnet. This open problem of understanding reversal processes in magnets with high spin values is not only of great theoretical interest but also is intimately connected to the development of modern technologies which are based on controlled switching of the spin state [9]. To this end, we perform an extensive numerical study of the general spin- s Ising and Blume-Capel models for various values of s . We investigate the underlying metastable behavior within the Becker-Döring theoretical framework, as well as Avrami's law.

The remainder of this manuscript is organized as follows: In the next section, we briefly review the Becker-Döring theory, and in Sec. III we introduce the models and the numerical scheme. In Sec. IV we present our results and scaling analysis. Finally, we end this contribution with a summary in Sec. V.

II. AN OVERVIEW OF CLASSICAL NUCLEATION AND DROPLET THEORY

Below the critical temperature T_c , if a very weak magnetic field (antiparallel to the initial spin direction) is applied to a ferromagnet, the system passes through a metastable state and then eventually decays to an equilibrium state. How long does the system remain in the metastable state? How does this state decay to the equilibrium state? What are the reversal mechanisms responsible for such a decay? All these questions are nicely explained by the classical nucleation and droplet

^{*}muktish.physics@presiuniv.ac.in

[†]nikolaos.fytas@coventry.ac.uk

theory, according to which in a spin-1/2 Ising system below T_c , small clusters or droplets of down spins are dispersed in the sea of up spins [1]. The number of such droplets with size l (l denotes the number of spins “-1”) is given by the Boltzmann distribution

$$n_l = N e^{-\beta E_l}, \quad (1)$$

where N is a normalization factor, $\beta = 1/k_B T$, k_B is the Boltzmann constant, T is the temperature, and E_l is the free energy of a droplet formation of size l . In fact, E_l comes from the contribution of bulk and surface energies,

$$E_l = -2hl + \sigma l^{(d-1)/d}, \quad (2)$$

where d is the space dimension, $-2hl$ corresponds to the bulk energy required to flip l number of spins in a magnetic field h , and the second term expresses the energy associated with the surface tension σ of the droplet. Historically, in classical nucleation theory, Allen-Cahn considered the Langevin equation of the droplet dynamics, which obviously involves the free energy. This is nicely reviewed in Ref. [1].

Classical nucleation theory [1,3] assumes that the droplets are mostly spherical-like in d -dimensional space. Thus, the radius of a droplet size l will be proportional to $\sim l^{1/d}$. The surface area will then be proportional to $\sim l^{(d-1)/d}$. Due to the opposite polarity of the two terms in Eq. (2), there is a competition between the two energies. As a consequence, there must be a critical size of the droplet l_c (with a radius R_c) for which the free energy is maximum, as given below,

$$l_c = \left(\frac{\sigma(d-1)}{2d|h|} \right)^d. \quad (3)$$

In the vicinity of the free-energy maximum, interesting dynamical phenomena are observed. Only the supercritical droplets having size $l > l_c$ will be energetically favored to grow (reducing the free energy) and eventually engulf the whole system, helping the reversal of magnetization. In contrast, the subcritical droplets ($l < l_c$) are found to shrink, reducing the free energy, and they are unable to take part in the reversal process. From this explanation of the droplet theory, it is obvious why the system consumes a certain period of time to leave the metastable state.

So the maximum energy associated with the critical size of the droplets is

$$E_l \Big|_{l=l_c} = E_c = \frac{K_d \sigma^d}{h^{d-1}}, \quad (4)$$

where $K_d = \frac{1}{d} \left(\frac{d-1}{2d} \right)^{d-1}$ is a d -dependent constant term. Now what is the growth rate of such droplets for different strengths of the applied field? This problem was analyzed by Becker and Döring [1,3]. The basic assumption of their analysis is that the time evolution of the number of droplets is only due to an evaporation-condensation mechanism in which a droplet either loses or gains a single spin without any type of coagulation or other interactions. The main result is that the number of droplets formed per unit time and volume (nucleation rate), I , is largely dependent on E_c ,

$$I = I_0 e^{-E_c/k_B T}, \quad (5)$$

where I_0 is the rate prefactor. Thus, the metastable lifetime in the nucleation regime, $\tau_{(nr)}$, can easily be obtained from the inverse nucleation rate I via

$$\tau_{(nr)} \sim I^{-1} \sim \exp \left(\frac{K_d \sigma^d}{k_B T h^{d-1}} \right). \quad (6)$$

As the applied-field strength is further increased, a different scenario for the reversal mechanism is observed: Many critical droplets grow simultaneously ($l^{1/d} \sim t$) and coalesce with each other, resulting in complete reversal of spins. Clearly, the rate of change in the magnetization is proportional to the droplet-size variation,

$$\frac{dm}{dt} \sim \frac{dl}{dt} \sim I t^d \rightarrow \Delta m \sim I \frac{\tau_{(cr)}^{d+1}}{d+1}, \quad (7)$$

where $\tau_{(cr)}$ is the metastable lifetime at the coalescence regime. So for a fixed change in the magnetization Δm , the metastable lifetime in the coalescence regime is

$$\tau_{(cr)} \sim I^{-\frac{1}{d+1}} \sim \exp \left(\frac{K_d \sigma^d}{k_B T (d+1) h^{d-1}} \right). \quad (8)$$

From the above description, and in particular from Eqs. (6) and (8), we can securely deduce that the metastable lifetime logarithm is described by a fair straight line when depicted as a function of the inverse applied-field strength. In addition to that, the slope of this line is expected to be smaller in the coalescence regime when compared to that in nucleation.

III. MODEL AND SIMULATION DETAILS

The spin- s Blume-Capel model [10], where s assumes integer or half-integer values of the spin, is described by the Hamiltonian

$$\mathcal{H} = -\frac{1}{s^2} J \sum_{(i,j)} s_i^z s_j^z + \frac{1}{s^2} \Delta \sum_i (s_i^z)^2 - \frac{1}{s} h \sum_i s_i^z, \quad (9)$$

where s_i^z denotes the z -component of the spin, which can take values from $-s$ to $+s$ through unit steps. For example, this means that for the $s = 5/2$ system, the normalized spin components $s_i^z = \{1, 3/5, 1/5, -1/5, -3/5, -1\}$ have been considered, instead of the usual $s_i^z = \{5/2, 3/2, 1/2, -1/2, -3/2, -5/2\}$. Obviously, for $s = 1/2$ and $\Delta = 0$ the original Ising model's Hamiltonian is recovered. Seven spin systems have been studied in the present work, namely the systems with $s = 1/2, 1, 3/2, 2, 5/2, 3$, and $7/2$. Returning to the description of Hamiltonian (9), we note the following: (i) The first term is the energy interaction between nearest-neighbor spins with uniform ferromagnetic coupling ($J > 0$). (ii) The second term models the single-ion anisotropy (or crystal-field coupling) Δ and controls the density of vacancies ($s_i^z = 0$) for the models with $s = 1, 2$, and 3 . (iii) The third term is the well-known Zeeman energy describing the interaction of an externally applied uniform magnetic field h along the z -direction with each individual spin. Both Δ and h have been measured in units of J , which sets the energy scale, and as usual we have set $J = k_B = 1$ to fix the temperature scale. Extensive results regarding the critical properties of the general spin > 1

Blume-Capel model can be found in the works by Plascak and collaborators [11,12]. For the particular spin-1 case, we refer the reader to Refs. [13–15].

All the numerical data shown in the following section were obtained via Monte Carlo simulations on a two-dimensional $L \times L$ square lattice, where $L = 100$, with periodic boundary conditions. As a side remark, we note here that the first and most extensive numerical work on the problem is due to Acharyya and Stauffer [4], in which sizes up to $L = 2048$ were simulated on the square-lattice Ising ferromagnet. In that work, a special technique, the so called multispin coding, was applied, where each bit of computer memory is filled by either 1 (for spins up) and 0 (for spins down). Moreover, a geometric parallelization was employed to facilitate the simulations, meaning that the whole lattice was divided into several strips and each strip was updated in different nodes of a CRAY-T3E supercomputer. However, in the present study of the general spin- s models, and in contrast to the spin-1/2 case, spin projections are not restricted to special values so that one cannot directly apply the method of multispin coding. In this respect, we consider the moderate size $L = 100$ as a fair compromise of the available computational facilities that will allow for a safe estimation of the properties under study; see also Ref. [16]. Of course, more extensive studies including larger system sizes would be welcome, but we believe that the main conclusions of our work will remain solid.

For the Blume-Capel models, we have fixed the single-ion anisotropy to $\Delta = 0.5$ throughout this work. Note that the locations of the tricritical points in the spin-1 and 3/2 models lie close to $\Delta_t \approx 1.966$ and 1.986, respectively [12,13]. Thus, we expect that $\Delta = 0.5$ is a reasonable choice for the current needs, since it guarantees that we stay well within the second-order transition regime of the phase diagram.

In our numerical protocol, the system is initially considered to be in the perfectly ordered state where all $s_i^z = +1$. Then a random updating scheme using the Metropolis single spin-flip algorithm is put into play, which follows the discrete time Markov chain based on the principle of detailed balance [17,18]. Let us briefly summarize the Metropolis algorithm's steps below:

(i) A lattice site is selected randomly among the $L \times L$ options.

(ii) The spin variable located at the selected site is flipped, keeping the other spins in the system fixed. The updated spin state may then be in any of the $2s + 1$ possible states between $-s$ and $+s$ which have been determined randomly with equal probability using the uniformly distributed random numbers between 0 and 1.

(iii) The energy change originating from this spin-flip operation is calculated using the Hamiltonian of Eq. (9) as follows: $\Delta\mathcal{H} = \mathcal{H}_a - \mathcal{H}_o$, where \mathcal{H}_a denotes the system's energy after the trial switch of the selected spin, and \mathcal{H}_o corresponds to the total energy of the old spin-configuration system. The probability to accept the proposed spin update is given by

$$W_M(s_i^z \rightarrow s_i^{z'}) = \begin{cases} \exp(-\Delta\mathcal{H}/k_B T) & \text{if } \mathcal{H}_a \geq \mathcal{H}_o, \\ 1 & \text{if } \mathcal{H}_a < \mathcal{H}_o. \end{cases} \quad (10)$$

(iv) If the energy is lowered, the newly chosen value of the spin projection is always accepted.

(v) If the energy is increased, a random number R is generated, such that $0 < R < 1$: If R is less than or equal to the calculated Metropolis transition probability, the selected spin is flipped. Otherwise, the old spin configuration remains unchanged.

This process corresponds to an update of a single spin. One Monte Carlo step per spin (MCSS) consists of a 10^4 number of such updates which act as the unit of time throughout this study. After the completion of each MCSS, the magnetization is determined via

$$m(t) = \frac{1}{N} \sum_{i=1}^N s_i^z, \quad (11)$$

where t is the time in units of MCSS and $N = L^2$ is the number of lattice points. The averaged magnetization is then calculated by $m(t)$ over the last 2×10^4 MCSS, where the first 5×10^3 steps are discarded during the thermalization process.

For the determination of suitable pseudocritical points, the lattice was allowed to evolve for 2.5×10^4 MCSS in the absence of any externally applied magnetic field. The pseudocritical temperatures were estimated from the peak location of the finite-lattice magnetic susceptibility curves χ , computed by the response function of the magnetization via $\chi = \beta N[\langle m^2 \rangle - \langle m \rangle^2]$. These estimates were found to be in good agreement with previous literature [16], as also discussed below.

Closing this section, we would like to make a few comments on the numerical approach and error estimation. Although the Metropolis algorithm may not be the optimum choice for studying critical properties of Ising and Blume-Capel models with higher spin-values [19,20], in the present work it is a safe and convenient vehicle, as we are only interested in the metastable behavior well below the critical point. Additionally, we expect the main conclusions of our work to be qualitatively insensitive to the use of other algorithms. At a quantitative level, however, the relaxation (or metastable) time can change depending on the chosen algorithm. For example, it is well-known that local- and cluster-update algorithms belong to different dynamic universality classes [21], and distinct values of metastable times should be expected. Finally, with respect to error estimation we have used the standard simple block averaging method [18]. Note that in some cases these error bars are not visible due to being of the order of symbol sizes.

IV. NUMERICAL RESULTS

The main aim of this paper is to understand the behavior of metastable states in spin- s Ising and Blume-Capel models. According to the Becker-Döring theory, the metastable state of the spin-1/2 Ising ferromagnet decays through the three different reversal mechanisms of the spin: strong-field regime, coalescence regime, and nucleation regime. These scenarios have been outlined above in Sec. II. Before presenting our main results, we would like to remind the reader that we mainly focus on the coalescence and nucleation regimes and attempt to provide some clear answers to the following open questions: Does the Becker-Döring analysis hold for the

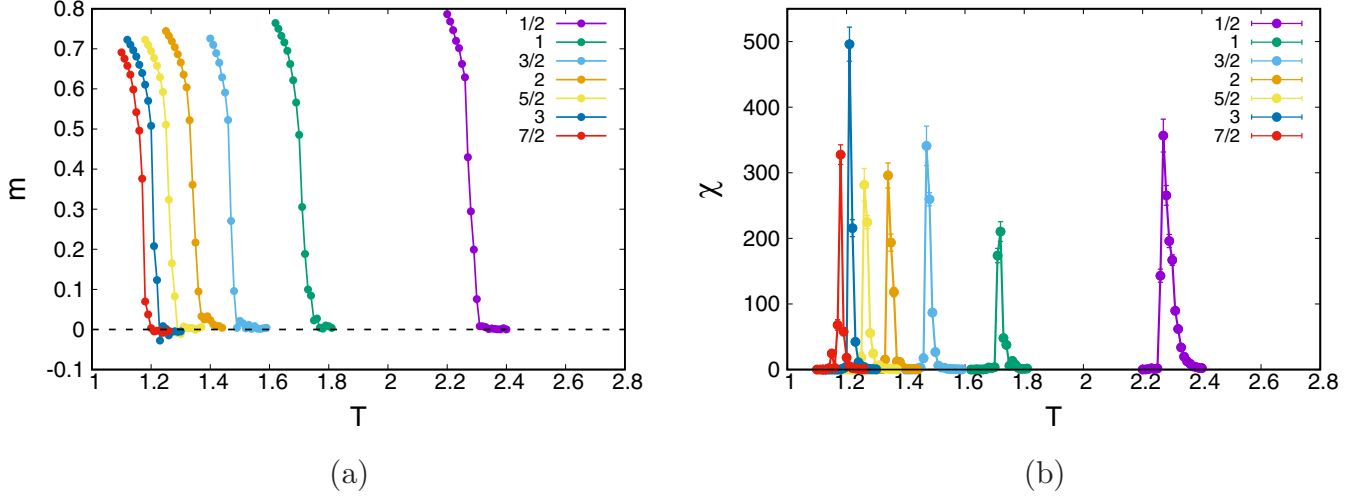


FIG. 1. Temperature dependence of the magnetization (a) and magnetic susceptibility (b) for the spin- s Ising models, where $s = 1/2, 1, 3/2, 2, 5/2, 3$, and $7/2$. Results averaged over 200 samples. In some of the data points, error bars are not visible as they are smaller than the symbol size.

general case of the spin- s Ising model? What are the effects of single-ion anisotropy?

Ideally, we would like to have a rough estimate of the critical temperature T_c of the normalized spin- s Ising and Blume-Capel models. The simplest way is to perform a finite-size scaling study based on the shift behavior of some suitably defined pseudocritical temperatures, T_L^* , i.e., those corresponding to susceptibility peaks [18,22]. However, the situation is much easier in the sense that we do not really need to know exactly T_c for each model. To explore the Becker-Döring theory, the system must simply be kept below the critical temperature, say around $\sim 0.7T_c$. Thus, if we simply consider the pseudocritical temperature of the susceptibility for a moderate system, this should be enough to ensure that the ratio $0.7T_L^* < T_c$. In this respect, we studied the variation of the equilibrium magnetization m and the corresponding susceptibility χ for both Ising and Blume-Capel systems, as shown in Figs. 1 and 2, respectively.

A few comments are in order: (i) The susceptibility was checked by varying the temperature in steps of $\delta T = 0.01$ so that the maximum error associated with the approximate T_L^* is of the order $\sim 10^{-2}$. In Table I a summary of approximate pseudocritical temperatures (considered up to second decimal place) is provided for the spin- s Ising and Blume-Capel models. For a direct comparison, note that a value $T_c(\Delta = 0.5) = 1.564(3)$ was obtained in Ref. [16] for the spin-1 Blume-Capel model. (ii) From Fig. 1 we observe that the critical temperature decreases with increasing s . In the spin-1/2 Ising system, the spin can either access the state “+1” or “−1.” As the number of spin components increases, the system walks through some intermediate accessible states between “+1” and “−1.” Then the activation energy needed to flip the spin from “+1” or “−1” via some intermediate state will be much smaller compared to the direct flipping. Furthermore, in the disordered state, the spin- s system will be equally distributed among all of its accessible states. For

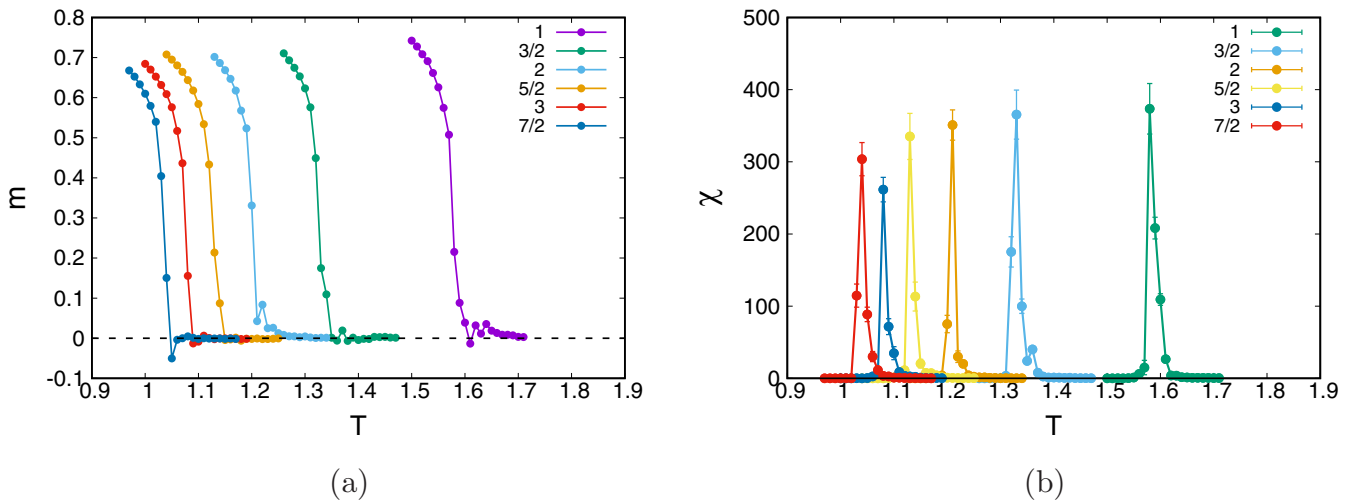


FIG. 2. The same as in Fig. 1 for the spin- s Blume-Capel models. Again, in some of the data points error bars are not discernible due to being smaller than the symbol size.

TABLE I. Pseudocritical temperatures of the $L = 100$ spin- s Ising and Blume-Capel models obtained from the peak location of the magnetic susceptibility. A uniform maximum error of 10^{-2} stems from the temperature-step $\delta T = 0.01$ in our simulations.

Spin- s systems s	Ising models $T_L^* (\Delta = 0)$	Blume-Capel models $T_L^* (\Delta = 0.5)$
1/2	2.27(1)	(not applicable)
1	1.72(1)	1.58(1)
3/2	1.47(1)	1.33(1)
2	1.34(1)	1.21(1)
5/2	1.26(1)	1.13(1)
3	1.21(1)	1.08(1)
7/2	1.18(1)	1.04(1)

these reasons, the system consumes lower energy (thermal activation-energy) to be driven into a fully disordered state. (iii) For the case of the Blume-Capel model, T_L^* is found to decrease in the presence of anisotropy compared to the spin- s Ising model. The presence of anisotropy favors energetically some of the intermediate states. Say, for example, for the spin-5/2 Blume-Capel model, normalized spin states “ $\pm 1/5$ ” will be more favored than “ $\pm 3/5$,” which are again more favorable than “ ± 1 ”—note that this statement is true for positive values of Δ , according to the description of Hamiltonian (1). So the thermal energy required to make an anisotropic system disordered is smaller compared to that needed for an isotropic Ising system.

Below the critical temperature, and if a very small magnetic field (in opposite direction to the spin moment) is applied to a ferromagnet, the system will enter into a metastable state with some positive magnetization. Then, after a certain period of time it will reach an equilibrium state through the decay of this metastable state. The time needed by the system to escape from the metastable state is known as the metastable lifetime, which is also referred to here as the reversal time τ of

the magnetization. Quantitatively, τ has been defined here as the time at which the magnetization changes sign [$m(t) \sim 0$]. In Fig. 3(a), we have checked the metastable lifetime of the spin- s Ising system in the presence of a small negative magnetic field $h = -0.4$ and at $T = 1.0$, which is well below the critical temperature of the spin-7/2 case, so that $T < T_c$ for all systems. The main observation here is that at a particular temperature, and in the presence of a uniform magnetic field, the reversal time is found to decrease with increasing s . This is due to the increase in the thermal fluctuations, which is connected to the fact that as we go to the higher spin values, T_c decreases and gradually approaches the fixed temperature $T = 1.0$. Similar results are presented also for the corresponding Blume-Capel models in Fig. 3(b) for the same magnetic field value and a temperature $T = 0.8$ as outlined in the figure.

Fixing now the temperature to $T = 0.7T_L^*$, we present in Fig. 4 a variation of the mean reversal time as a function of the inverse magnetic field for the spin-1/2, -2, -5/2, and -3 Ising models. Three different regimes with distinct slopes are clearly identified (see also the discussion in the figure panels). For the fits shown, we have implemented the standard χ^2 test for goodness of fit. Specifically, the p value of our χ^2 test, also known as Q (see, e.g., Ref. [23]), is the probability of finding a χ^2 value that is even larger than the one actually found from our data. Recall that this probability is computed by assuming (i) Gaussian statistics and (ii) the correctness of the fit’s functional form. We consider a fit as being fair only if $10\% < Q < 90\%$. In Table II the results with respect to the quality of our fits are given and provide a strong credibility test.

Qualitatively one can clearly argue that the Becker-Döring analysis holds for the general spin- s Ising systems studied. An interesting point is that, although each system is kept at $T = 0.7T_L^*$, the metastable lifetime rises for $s > 1/2$ [see Figs. 4(b)–4(d)] with respect to that for $s = 1/2$ [see Fig. 4(a)]. As we discussed previously, systems with $s > 1/2$

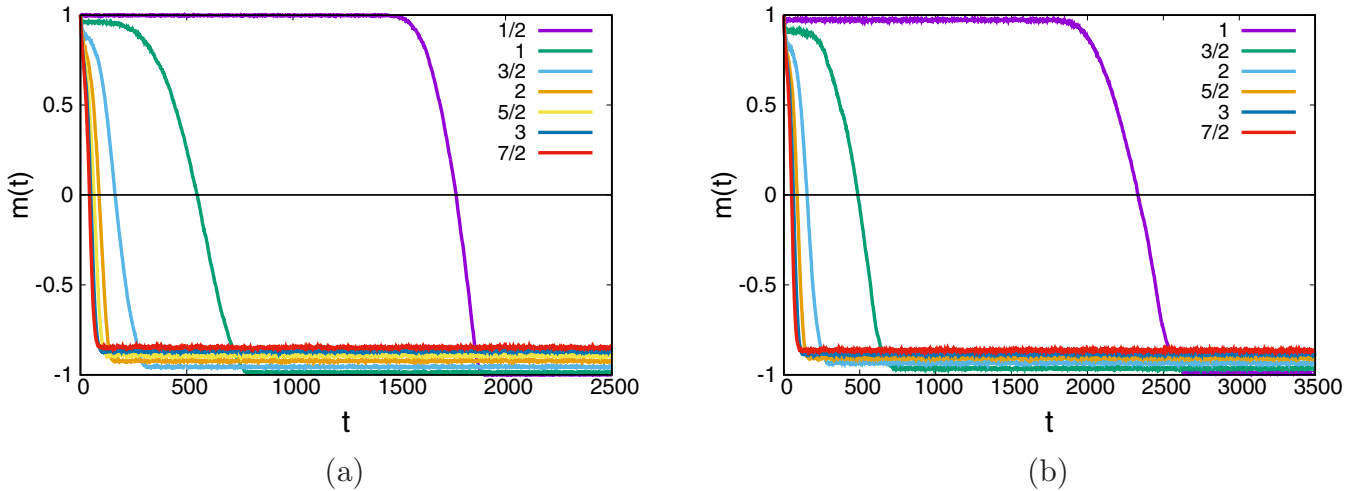


FIG. 3. (a) Variation of the magnetization with time (in MCSS) for Ising models at $T = 1.0$ and $h = -0.4$. Reversal times for the spin- $\{1/2, 1, 3/2, 2, 5/2, 3, 7/2\}$ systems are $\tau = 1767, 549, 163, 87, 63, 48$, and 42 MCSS, respectively. (b) Analogous results for Blume-Capel models at $T = 0.8$ and $h = -0.4$. Reversal times for the spin- $\{1, 3/2, 2, 5/2, 3, 7/2\}$ systems are $\tau = 2332, 487, 153, 88, 63$, and 51 MCSS, respectively. In both panels, typical benchmark curves obtained from a single run are shown for illustrative reasons.

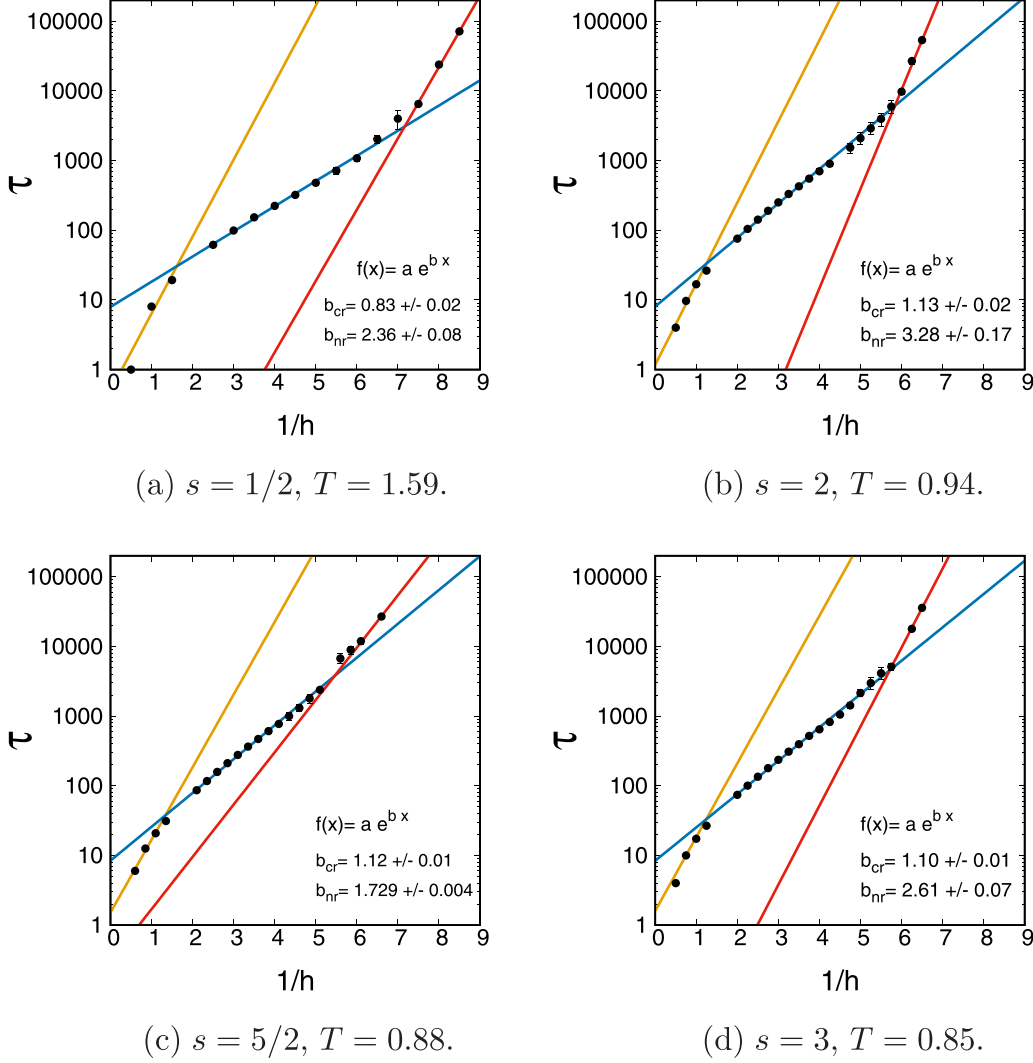


FIG. 4. Mean reversal time as a function of the inverse magnetic field at $T = 0.7T_L^*$ for four spin- s Ising models, as indicated in the panels. Results averaged over 1000 samples. In cases in which the error bars are not visible, this is due to being smaller than the symbol size used. Note the appearance of three different regimes: (i) strong-field regime (yellow line), (ii) coalescence regime (blue line), and (iii) nucleation regime (red line), which are identified with different slopes. Note the logarithmic scale in the vertical axis. See also Table II.

have some intermediate states between “+1” and “−1.” Now if we go back to the droplet theory, the bulk energy term in Eq. (2) will be modified for the spin- $s > 1/2$ case, since the

TABLE II. Fitting parameters corresponding to Fig. 4. We have used the standard χ^2/DOF test for goodness of fit, where DOF denotes the number of degrees of freedom. Specifically, the Q value of our χ^2 tests is the probability of finding a value of χ^2 larger than the one actually found from our numerical data—see also the relevant discussion in the main text.

Spin- s systems	Coalescence regime			Nucleation regime		
	χ^2	DOF	Q	χ^2	DOF	Q
1/2	6.5798	7	0.4739	3.7075	2	0.1566
2	17.0516	12	0.1477	3.4113	2	0.1816
5/2	13.5384	12	0.3311	4.9426	3	0.1761
3	16.5078	13	0.2228	0.1689	1	0.6811

energy needed to flip the droplet of some intermediate state will be less than that needed to flip the droplet of spin “+1.” The droplet’s formation-energy will then be $E_l = -ahl + \sigma l^{(d-1)/d}$, where $0 < a \leq 2$. Obviously, $a = 2$ corresponds to the spin-1/2 Ising system. Thus, the critical droplet size will be $l_c = [\sigma(d-1)/(ad|h|)]^d$. Clearly, the critical size l_c becomes larger for systems with $s > 1/2$ resulting in longer times needed for the system to escape the metastable state. Also, the d -dependent constant term K_d increases since the denominator factor 2 in Eq. (3) will be replaced by a . Finally, from Eqs. (6) and (8) it can be confirmed also that the reversal time increases.

An analogous illustration is presented in Fig. 5 for the anisotropic spin- s Blume-Capel model with $s = 3/2, 2, 5/2$, and 3. The obtained results indicate that the Becker-Döring analysis of three different reversal spin mechanisms is again verified. One minor comment here is that for a particular s -value, the reversal time of the spin- s Blume-Capel model is found to decrease in comparison to the Ising case. Actually,

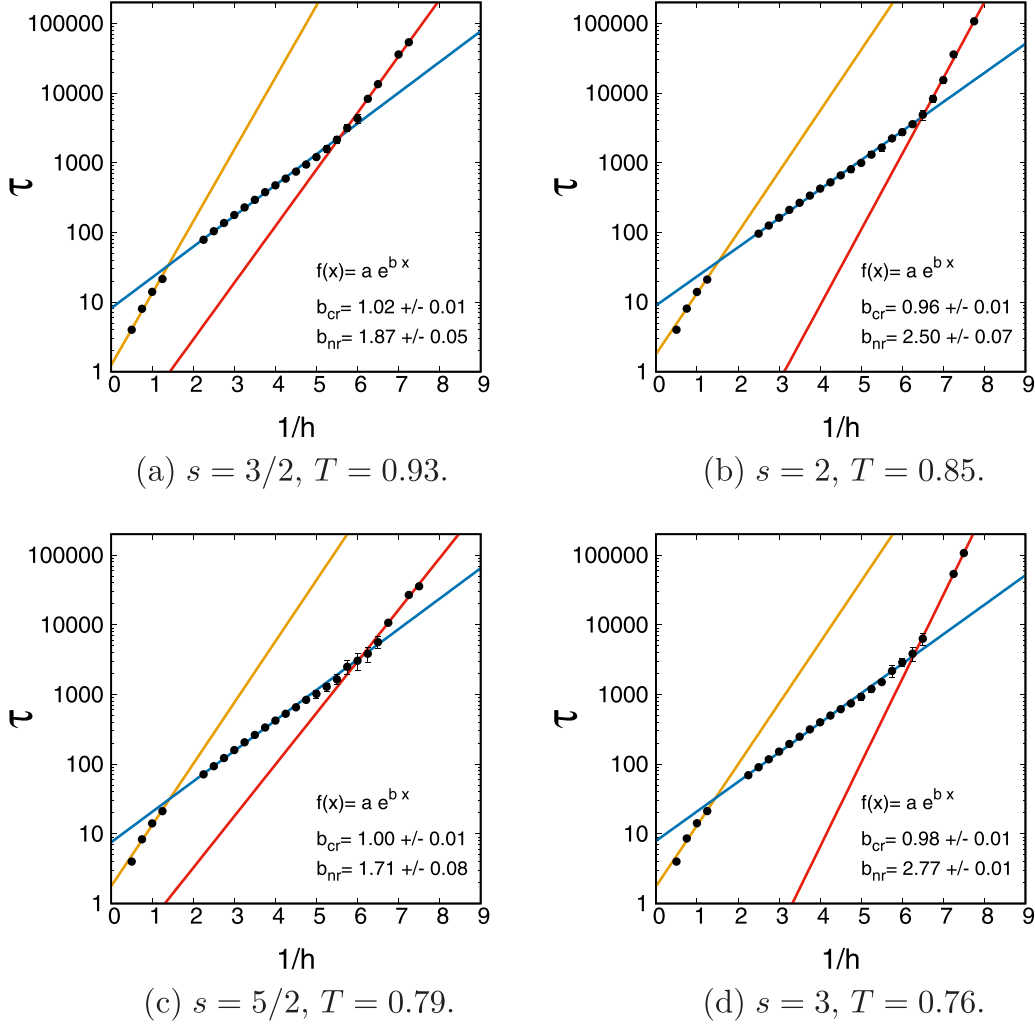


FIG. 5. Same as in Fig. 4 for four spin- s Blume-Capel models. Again, in some of the data points error bars are smaller than the symbol size. See also Table III.

due to the presence of anisotropy, some of the states will be energetically more favorable so that the effective bulk energy in Eq. (2) will be increased, causing the decrease in l_c as well in the metastable lifetime. This phenomenon has also been reported very recently in Ref. [6]. Table III gives a descriptive summary of our statistical tests corresponding to Fig. 5, again in favor of our approach.

At this stage, the time dependence of the metastable volume fraction decay is crucial in order to obtain an idea about

the spin dynamics of our problem. According to Avrami's law [7], the logarithm of the metastable volume fraction in a d -dimensional Ising system decays as $\sim t^{d+1}$ close to T_c . This behavior has already been verified in the two-dimensional random-field Ising model [5] and the spin-1 Blume-Capel model [6]. Here we have checked the validity of this law for the spin-7/2 Ising system at $T = 0.7T_L^*$; see Fig. 6. We considered the relative abundance of the 7/2, 5/2, 3/2, and 1/2 states as the metastable volume fraction, and also their total relative abundance is presented (black line in Fig. 6). The results indicate that Avrami's law in the spin-7/2 Ising system is well obeyed. In addition, under the influence of a weak field the logarithm of the volume fraction decays faster in the vicinity of the metastable lifetime $(t/\tau)^3 = 1$ compared to later times. On the other hand, in the presence of strong fields the decay rate is higher at $t > \tau$. Additionally, a peak at the initial stage is observed for the density of $s_i^z = 5/2, 3/2$, and $1/2$. This should be expected because initially the 7/2 state will decay into those states which will then decay to other subsequent ones, i.e., $s_i^z = -1/2, -3/2$, and $-5/2$. In full analogy to Fig. 6, Fig. 7 is a manifestation

TABLE III. Fitting parameters corresponding to Fig. 5.

Spin- s systems	Coalescence regime			Nucleation regime		
	χ^2	DOF	Q	χ^2	DOF	Q
3/2	11.3564	13	0.581	3.9435	3	0.2676
2	11.322	14	0.6606	3.9403	3	0.268
5/2	13.3257	14	0.5010	5.5415	3	0.1362
3	16.3331	14	0.2934	0.4569	2	0.7958

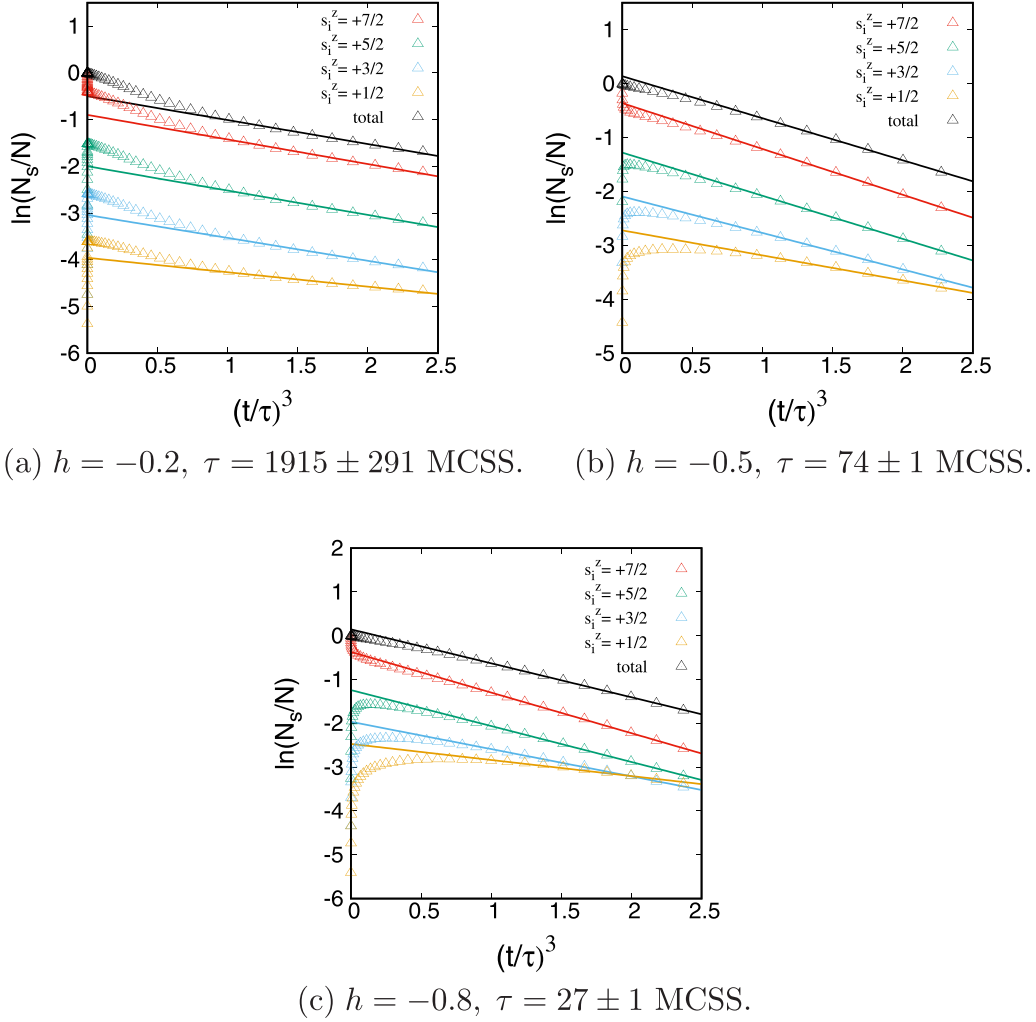


FIG. 6. Variation of $\ln(N_s/N)$ of the spin components $s_i^z = \{7/2, 5/2, 3/2, 1/2\}$ and also of the total vs $(t/\tau)^3$ for the $s = 7/2$ Ising system in the presence of three different strengths of the applied field. N_s is the number of particular spin state s_i^z , N is the total number of spins, and τ is the reversal time. For the case of black open triangles, N_s is the total number of the four spin components. The temperature is set to $T = 0.7T_L^*$ and the fits shown by the solid lines correspond to times $t > \tau$. Results averaged over 1000 samples are shown with the size of error bars being smaller than that of the symbol size used.

of Avrami's law for the anisotropic spin-5/2 Blume-Capel model.

V. SUMMARY

In summary, we have investigated the metastable behavior of general discrete spin- s models. Classical nucleation theory, as proposed by Becker and Döring many years ago, has been nicely verified in a number of recent studies for the spin-1/2 Ising ferromagnet. However, it was still unclear whether the theory accommodates metastability phenomena of general spin- s ferromagnetic models. Other open questions under scrutiny include the effect of single-ion anisotropy on the reversal time of the magnetization and decay of the metastable volume fraction. We believe that these questions have been satisfactorily addressed in the current paper.

In particular, our Monte Carlo results for the general Ising and Blume-Capel models fully verified predictions of the

Becker-Döring theory, indicating its wide applicability to the general case of spin- s ferromagnetic models. Redefining the metastable volume as the relative abundance of the positive values of the spin projections, we studied its variation as a function of the time for three different regimes of the applied magnetic field (weak, intermediate, and strong). In all cases, the metastable volume fraction was found to decay following Avrami's law. Finally, many of the intriguing phenomena revealed via Monte Carlo simulations were explained using simple energetic arguments of droplet formation in the underlying theory.

Altogether, as became apparent from this work, the system becomes more flexible for reversal as the value of s increases. At this stage, it would be very interesting to investigate the reversal mechanisms for continuous spin Ising and Blume-Capel models, possibly determining the limit of flexibility in these reversal processes. In any case, the technological importance of using magnets with higher spin values for magnetic recording and switching has been highlighted very recently

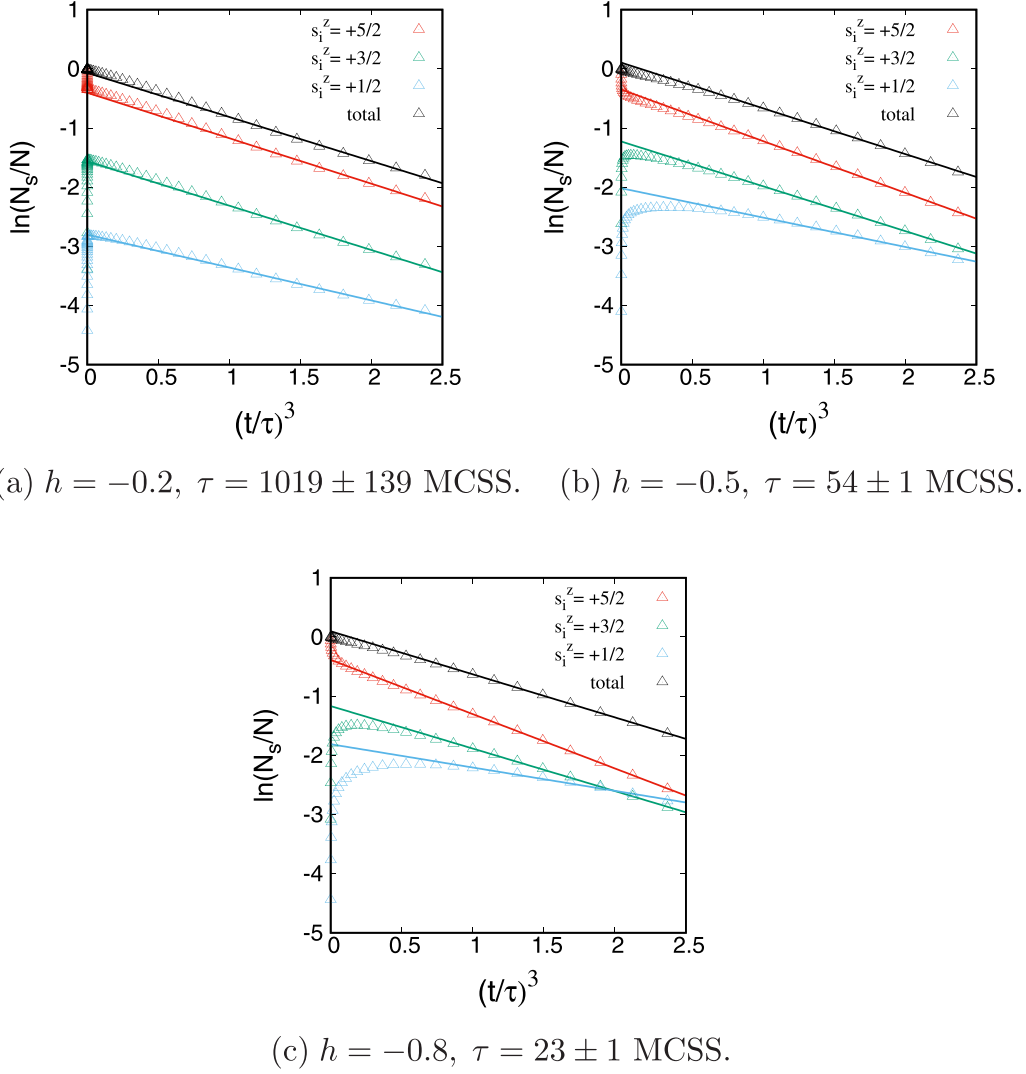


FIG. 7. Similar to Fig. 6 for the spin components $s_i^z = \{5/2, 3/2, 1/2\}$ and also for the total of them for the $s = 5/2$ Blume-Capel model. Again, as in Fig. 6, the size of error bars is smaller than the symbol size.

in Ref. [9], and we hope that this work will pave the way for more advanced studies in this growing field of research. Note that the Blume-Capel model considered in this work has been widely used up to now in the literature for modeling various physical systems with experimental analogs in and out of equilibrium; see Ref. [15] and references therein. Other fruitful candidates would be the general q -states Potts model and the anisotropic Heisenberg ferromagnet (having continuous spin symmetry) where compelling metastability results are expected while varying the number of spin states q and anisotropy. We plan to pursue these research avenues in the near future.

ACKNOWLEDGMENTS

We would like to thank the two anonymous referees who have helped us improve our manuscript with their instructive comments. M.N. would like to thank the Swami Vivekananda Scholarship (SVMCMS) for financial support. M.A. acknowledges financial support from the FRPDF grant of Presidency University. We would also like to thank A. Mukherjee for her suggestion on common online Latex editing. The numerical calculations reported in this paper were performed at TÜBİTAK ULAKBİM, High Performance and Grid Computing Center (TR-Grid e-Infrastructure).

- [1] J. D. Gunton and M. Droz, *Introduction to the Theory of Metastable and Unstable States* (Springer-Verlag, Berlin, 1983).
- [2] S. N. Piramanayagam and T. C. Chong, *Development in Data Storage: Material Perspective* (Wiley-IEEE, 2011).

- [3] R. Becker and W. Döring, *Ann. Phys. (Leipzig)* **24**, 719 (1935).
- [4] M. Acharyya and D. Stauffer, *Eur. Phys. J. B* **5**, 571 (1998).
- [5] M. Naskar and M. Acharyya, *Physica A* **551**, 124583 (2020).

- [6] M. Naskar and M. Acharyya, *Eur. Phys. J. B* **94**, 36 (2021).
- [7] M. Avrami, *J. Chem. Phys.* **7**, 1103 (1939); **8**, 212 (1940); **9**, 177 (1941).
- [8] M. Naskar and M. Acharyya, *Physica A* **568**, 125747 (2021).
- [9] S. Shankar *et al.*, *Nat. Commun.* **9**, 4750 (2018).
- [10] M. Blume, *Phys. Rev.* **141**, 517 (1966); H. W. Capel, *Physica (Amsterdam)* **32**, 966 (1966); **33**, 295 (1967); **37**, 423 (1967).
- [11] J. A. Plascak, J. G. Moreira, and F. C. sá Barreto, *Phys. Lett. A* **173**, 360 (1993).
- [12] J. A. Plascak and D. P. Landau, *Phys. Rev. E* **67**, 015103(R) (2003).
- [13] J. Zierenberg, N. G. Fytas, M. Weigel, W. Janke, and A. Malakis, *Eur. Phys. J. Spec. Top.* **226**, 789 (2017).
- [14] N. G. Fytas, J. Zierenberg, P. E. Theodorakis, M. Weigel, W. Janke, and A. Malakis, *Phys. Rev. E* **97**, 040102(R) (2018).
- [15] E. Vatansever, Z. Demir Vatansever, P. E. Theodorakis, and N. G. Fytas, *Phys. Rev. E* **102**, 062138 (2020).
- [16] A. Malakis, A. N. Berker, I. A. Hadjiagapiou, N. G. Fytas, and T. Papakonstantinou, *Phys. Rev. E* **81**, 041113 (2010).
- [17] N. Metropolis, A. W. Rosenbluth, M. N. Rosenbluth, and A. H. Teller, *J. Chem. Phys.* **21**, 1087 (1953).
- [18] D. P. Landau and K. Binder, *A Guide to Monte Carlo Simulations in Statistical Physics* (Cambridge University Press, Cambridge, UK, 2000).
- [19] S. Bekhechi and A. Benyoussef, *Phys. Rev. B* **56**, 13954 (1997).
- [20] J. A. Plascak, A. M. Ferrenberg, and D. P. Landau, *Phys. Rev. E* **65**, 066702 (2002).
- [21] M. E. J. Newman and G. T. Barkema, *Monte Carlo Methods in Statistical Physics* (Oxford University Press, New York, 1999).
- [22] A. M. Ferrenberg and D. P. Landau, *Phys. Rev. B* **44**, 5081 (1991).
- [23] W. H. Press, S. A. Teukolsky, W. T. Vetterling, and B. P. Flannery, *Numerical Recipes in C*, 2nd ed. (Cambridge University Press, Cambridge, 1992).